Rúbia Young Sun Zampiva
Researcher
Federal University of Rio Grande do Sul
Department of Materials Engineering
Brazil

Claudir Gabriel Kaufmann Jr
Researcher
Federal University of Rio Grande do Sul
Department of Materials Engineering
Brazil

Annelise Kopp Alves
Professor
Federal University of Rio Grande do Sul
Department of Materials Engineering
Brazil

Carlos Pérez Bergmann
Professor
Federal University of Rio Grande do Sul
Department of Materials Engineering
Brazil

Influence of the Fuel Composition and the Fuel/Oxidizer Ratio on the Combustion Solution Synthesis of $MgFe_2O_4$ Catalyst Nanoparticles

Solution combustion synthesis (SCS) has been widely applied to produce oxide catalysts due to the possibility of producing highly pure and hom–ogeneous nanostructured powders at low cost. The smaller the particles are and the higher the surface area is, the more efficient the powder catalyst will be. For iron-based catalysts such as ferrites, the degree of spinel inversion is another factor that affects the catalyst activity. In SCS, the particle size, surface area, and degree of spinel inversion are fundamentally related to process variables such as the fuel composition and the fuel/oxidizer ratio. Therefore, we studied the application of glycine and polyethylene glycol - 200 molecular weight (PEG 200) as fuels and the influence of the fuel/oxidizer ratio in the SCS of $MgFe_2O_4$ catalyst nanoparticles. The products' morphology and composition were systema–tically characterized by X-ray diffraction, microscopy analyses, and specific surface area. The results indicate the production of high-purity nanoparticles with increased surface area, which was obtained with low concentrations of glycine and a wide range of particle sizes that depend on the fuel composition and concentration.

Keywords: *SCS, $MgFe_2O_4$, nanostructured materials, catalyst*

1. INTRODUCTION

Nanoscience has become a focus in several research areas due to the different material properties that occur at the nanometer scale. For example, in nanostructured form, some materials become exceptionally strong, hard, or ductile at high temperatures. These charac–teristics are controlled by the size, composition, and morphology of the material [1-5]. Nanostructured catalysts have high efficiency because the large surface area of the particles provides greater availability to carry out catalysis [6, 7]. The smaller the particle diameter, the greater the number of atoms exposed on the surface. The diameter, purity, and homogeneity of the catalyst are crucial for the yield of the reactions in which they are employed [8].

Many studies on ferrites nanoparticles including $MgFe_2O_4$ spinel have been recently described due to their distinct magnetic properties, which open up numerous application possibilities including cancer treatment [9, 10], biosensors [11], memory shape alloys [12] and water purification [13]. $MgFe_2O_4$ has also been used as a catalyst in the production of carbon structures such as carbon nanotubes (CNT). In CNT studies, spinels are usually based on metal catalysts (Ni, Co, Mo, Fe,...) and are supported by oxides (MgO, Al_2O_3, SiO_2, and CaO) [14-16]. Magnesium ferrite spinel is an excellent catalyst for multiwall CNT (MWCNT) production. $FeMg_2O_4$ when applied as a catalyst is often represented in the literature by Fe/MgO system [17-20] because metallic Fe^{3+} ions are the active catalyst in the synthesis process, while MgO acts as the dispersant of Fe^{3+} ions (support) [19].

Magnesium ferrite ($MgFe_2O_4$) is also applied in other processes, such as dehydrogenation, oxidation, and alkylation reactions [20]. In addition to the surface area, the position of the iron ions in the $MgFe_2O_4$ structure has a significant influence on the catalyst's efficiency. $MgFe_2O_4$ has a spinel structure, with Mg occupying the tetrahedral sites and Fe occupying the octahedral sites. These ions can change sites with each other and invert the spinel order, depending on the method applied to produce the catalyst. This inversion allows for a higher quantity of iron on the crystallite surfaces due to the position of the tetrahedral sites. Inversion of the spinel position directly affects the physicochemical properties of the ferrite [21-22]. Since magnesium has a covalent character and oxygen has negligible mobility, iron has the highest mobility in the magnesium ferrite structure [23, 24].

Figure 1 presents the spinel ferrite Fd-3m cubic structure. In a normal spinel structure, the divalent (A^{II}) ions occupy tetrahedral sites, and the trivalent (B^{III}) ions occupy the octahedral sites in a close packed arrangement of oxide ions.A normal spinel can be represented as $(A^{II})^{tet}(B^{III})_2{}^{oct}O_4$. In an inverse spinel structure, the A^{II} ions occupy the octahedral sites, and part of the B^{III} ions occupy the tetrahedral sites. This can be represented as $(B^{III})^{tet}(A^{II}B^{III})^{oct}O_4$[25].

Received: March 2017, Accepted: November 2017
Correspondence to: Dr. Rúbia Young Sun Zampiva
Federal University of Rio Grande do Sul- UFRGS.
Osvaldo Aranha 99, Porto Alegre, RS 90035, Brazil
E-mail: rubiayoungsun@gmail.com
doi:10.5937/fmet1802157Z

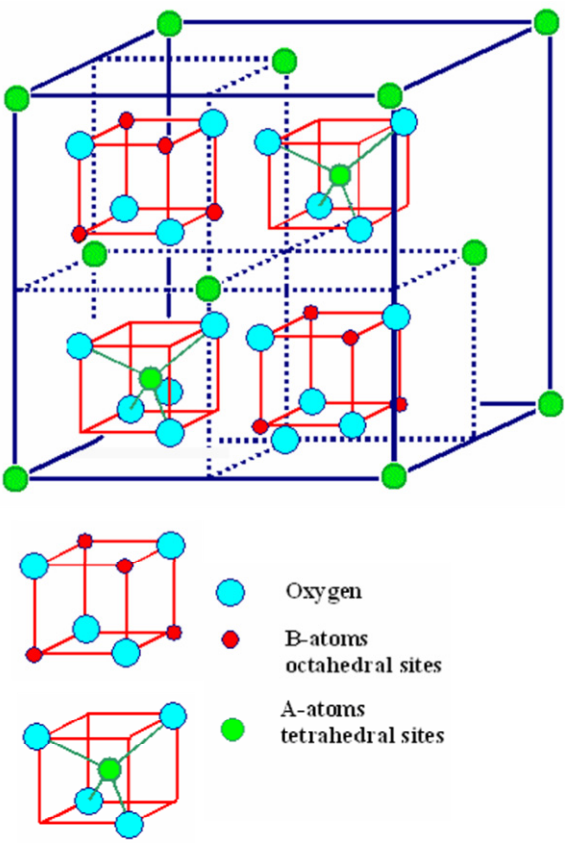

Figure 1. AB_2O_4 Spinel; The red cubes are also contained in back half of the unit cell. The spinel structure of ferrites is shown indicating the tetrahedral and octahedral sites. Adapted from [26].

Solution combustion synthesis (SCS) has been increasingly applied in the production of oxide catalysts due to the possibility of producing low-cost, highly pure, and homogeneous nanostructured powders. SCS mainly consists of combining the reactants in an aqu–eous medium using a complexing agent (fuel) such as citric acid [27], oxalic acid [28, 29], glycine [30, 31], and urea [32], as well as oxidizing agents (usually metal nitrates), to oxidize the fuel [34, 35]. The mixture is heated to 150°C and 500°C to carry out self-sustaining ignition in a rapid combustion reaction that can reach more than 1700°C [36]. A solid product that is typically unagglomerated and crystalline is formed at the end of the process [36]. The distribution of the ions throughout the crystal structure is uniform due to the atomic mixing of the reactants in the initial solution [38].

In the SCS synthesis of spinels, the enthalpy and flame temperature generated during combustion mainly govern the powder characteristics, such as the crystallite size, surface area, nature of agglomeration (strong vs. weak), and the degree of spinel inversion [40]. These properties are mainly adjusted by controlling the chemical composition of the fuel and the ratio of fuel to the oxidizer ratio [41]. The stoichiometry of the SCS reactions is determined based on calculations for fuel-oxidizer mixtures in the chemistry of propellants [39-41], which consider the amount of oxidizing and reducing elements in the reaction [42].

Previous studies showed that the stoichiometric ratio is not always the most efficient [42]. Thus, this study aims to formulate a methodology to use SCS to produce homogeneous $MgFe_2O_4$ catalyst nanoparticles with high surface area and degree of spinel inversion. For this purpose, we studied the application of glycine and polyethylene glycol - 200 molecular weight (PEG 200) as fuels, as well as the influence of the fuel/oxidizer ratio in the SCS of $MgFe_2O_4$ catalyst nanoparticles.

2. MATERIALS AND METHODS

2.1 Synthesis of $MgFe_2O_4$ particles

$MgFe_2O_4$nanostructured particles were produced by SCS with various compositions and concentrations of fuel. $Mg(NO_3)_2.6H_2O$ and $Fe(NO_3)_3.9H_2O$ were emplo–yed as precursors and oxidizers, while glycine ($C_2H_5NO_2$) and Polyetileneglicol- PEG 200 ($H(OCH_2CH_2)_nOH$) were used as fuels. All of the reactants were obtained from Merck. The fuel rich, stoichiometric and lean ratios were established by the chemistry of pro–pellants method [43] and applied according to Equations 1, 2 and 3 for glycine; and equations 4, 5 and 6 for PEG, respectively.

Glycine Fuel:

Fuel rich reaction (AG1):

$$2\ Fe(NO_3)3.9\ H_2O + Mg(NO_2)3.6\ H_2O + \\ +6.33\ C_2H_5NO_2 + 4.24\ O_2 \rightarrow MgFe_2O_4 + 7.66\ N_2 + \\ +12.66\ CO_2 + 39.82\ H_2O \quad (1)$$

Fuelstoichiometric (AG2):

$$2\ Fe(NO_3)3.9\ H_2O + Mg(NO_2)3.6\ H_2O + \\ +\ 5.33\ C_2H_5NO_2 + 1.93\ O_2 \rightarrow MgFe_2O_4 + 7.16\ N_2 + \\ +\ 10.\ 6\ CO_2 + 37.32\ H_2O \quad (2)$$

Fuel lean (AG3):

$$2\ Fe(NO_3)3.9\ H_2O + Mg(NO_2)3.6\ H_2O + \\ +\ 4.33\ C_2H_5NO_2 \rightarrow MgFe_2O_4 + 6.66\ N_2 + 12.66\ CO_2 \\ +\ \ 34.82\ H_2O + 0.52\ O_2 \quad (3)$$

PEG Fuel:

Fuel rich reaction (AP1):

$$2\ Fe(NO_3)3.9\ H_2O + Mg(NO_2)3.6\ H_2O + \\ +\ 2.7\ H(OCH_2CH_2)4.7\ OH + 17.94\ O_2 \rightarrow MgFe_2O_4 + \\ +\ \ 4.5\ N_2 + 21.6\ CO_2 + 52.08\ H_2O \quad (4)$$

Fuel stoichiometric reaction (AP2):

$$2\ Fe(NO_3)3.9\ H_2O + Mg(NO_2)3.6\ H_2O + \\ +\ 1.7\ H(OCH_2CH_2)4.7\ OH + 9.97\ O_2 \rightarrow MgFe_2O_4 + \\ +\ \ 4.5\ N_2 + 15.98\ CO_2 + 41.68\ H_2O \quad (5)$$

Fuel lean (AP3):

$$2\ Fe(NO_3)3.9\ H_2O + Mg(NO_2)3.6\ H_2O + \\ +\ 0.7\ H(OCH_2CH_2)4.7\ OH \rightarrow MgFe_2O_4 + 4.5\ N_2 + \\ +\ 6.58\ CO_2 + 31.28\ H_2O + 1.77\ O_2 \quad (6)$$

The nitrates were individually dissolved in water and then mixed. The solution was stirred and heated for approximately 5 min. When reaching 60°C, the fuel that had previously been dissolved in water was added to the solution. The temperature was maintained under stirring for a few minutes to promote perfect homogenization. The solution was placed in an electric muffle furnace

preheated to 400°C until complete combustion (around 15 min). The samples were heat treated at 1100°C, and no grinding process was applied.

2.2 Chemical and structural characterization

The crystallinity of the samples was evaluated by X-ray diffraction (XRD) using a PHILIPS diffractometer (model X'Pert MPD) at 40 kV and 40 mA using a Cu anode. The powder crystallite sizes were calculated using Scherrer's equation:

$$D_p = \frac{K\lambda}{\beta_{1/z}\cos\theta} \quad (7)$$

where D represents the crystallite size, K is a constant that depends on the particle shape (we assume the particles to be spherical, meaning K=0.94), λ is the wavelength of the electromagnetic radiation used (1.5406 Å, a value related to the main characteristic radiation emitted by copper), θ is Bragg`s angle, and β is the contribution of the crystallite size to the full width at half maximum (FWHM) of the corresponding diffraction peak in radians.

The surface areas of the catalysts were obtained by the nitrogen adsorption method (BET - Quanta Chrome, Nova-1000 model). The morphology of the $MgFe_2O_4$ was characterized by scanning electron microscopy (SEM) using a JEOL microscope (JSM 6060) with a maximum operating voltage of 30 kV and a nominal resolution of 3.5 nm. The applied voltage was 10 to 20 kV. Transmission electron microscopy (TEM) was also carried out using a JEOL microscope (JEM 1200 EXII model) operating between 80 and 100 kV with a point resolution of 0.45 nm and line resolution of 0.20 nm. The powder sample was placed on a Cu grid and coated with a carbon film, to avoid magnetic interactions with the TEM microscope.

3. RESULTS

The diffractograms in Figure2 shows the characteristic crystal peaks corresponding to the magnesioferrite phase for all samples according to JCPDS 73-1960. The samples produced with glycine (AG1, AG2, and AG3) presented a high degree of purity and showed only the $MgFe_2O_4$ phase.

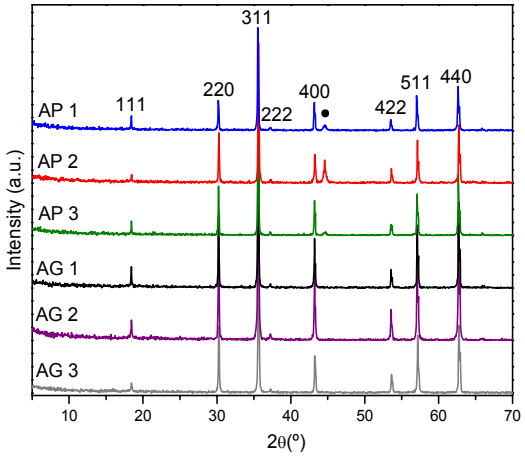

Figure 2. Diffractograms of the $MgFe_2O_4$ catalysts for different fuel compositions and concentrations.

In addition to the $MgFe_2O_4$ peaks, the samples produced with PEG (AP1, AP2, and AP3) show a small peak at 44.61° related to periclase formation (MgO, JCPDS 07-0239). All samples presented a 111 peak related to the degree of spinel inversion [45]. A higher intensity of this peak compared to the [311] peak indicates a higher degree of spinel inversion [45].

Figure 3 presents the difference in intensity between the [111] and [311] peaks. The samples produced with PEG showed a smaller difference than the glycine samples, indicating a higher degree of spinel inversion in these samples.

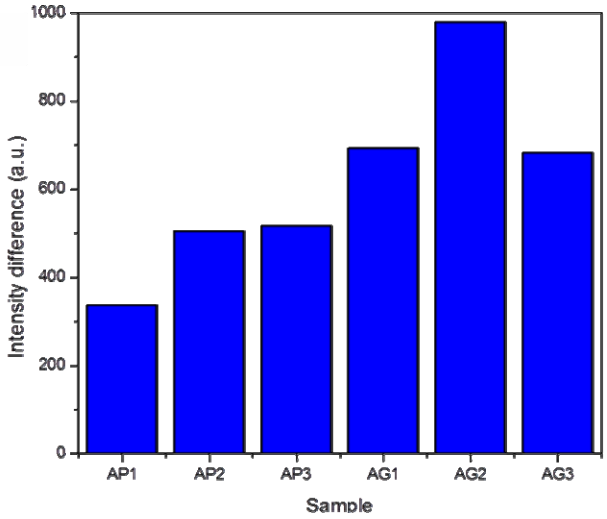

Figure 3. a) Difference between the [111] and [311] peak intensities. The smaller the difference, the higher the degree of spinel inversion.

The crystallite sizes calculated by Scherrer`s equation are shown in Figure4. The samples prepared with PEG had similar sizes around 58 nm, while the samples prepared with glycine showed different sizes for the different concentrations: 58.12 nm for AG1, 48.43 nm for AG2, and 45.88 nm for AG3 (the smallest size among all samples). According to the XRD analysis, the samples produced with glycine presented the highest purity and smallest crystallite size, while the samples prepared with PEG presented the highest degree of spinel inversion. Independently of the fuel concentration and composition, which directly affects the temperature of heat treatment, the crystallite size remained at the scale of dozen nanometers.

This phenomenon is related to the covalent character of magnesium, which makes crystallization more difficult and leads to smaller crystallites [46].

Surface area is one of the most important parameters in catalytic nanoparticles. Large surface areas provide more active ions for catalysis and increase reaction rates [47, 48]. Particles are composed of 2 or more single crystals (crystallites). The total surface area of a particulate sample and the size of the crystallites in the particles are usually inversely proportional. Smaller crystallites form smaller particles with higher surface area. Nanoparticles tend to agglomerate and form larger particles with less surface area.The values presented in table 1, for the samples surface area, are in agreement with the crystallite sizes presented in Figure 4. The increasing crystallite size from sample AG3 to AP1 decreased the samples surface area.

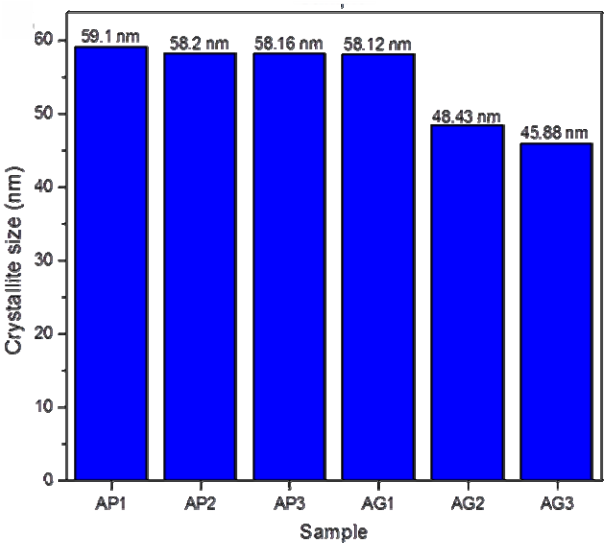

Figure 4. Mean crystallite size calculated by Scherrer`s equation based on the diffractograms.

Table 3. Powder catalyst surface areas based on fuel composition and concentration in SCS.

Sample	Surface area (m^2/g)
AP1	4,178
AP2	13,579
AP3	16,077
AG1	13,149
AG2	25,160
AG3	34,650

The surface areas of the spongy structures are also in agreement with the results observed by SEM (Figure 5 for the samples produced using glycine and Figure 6 for the samples produced with PEG) where the catalysts AG3 and AG2 (Figures c and b) presented the highest surface area, while AP1 and AP2 (Figure 5 a and b) were the densest samples. As the fuel concentration increased for both compositions, the surface area of the catalysts decreased, as did the mean crystallite size of the powders, as shown in Figure4.

Figure 5 and 6 shows SEM micrographs of the $MgFe_2O_4$ samples just after calcination with no grinding process involved. The powders appeared spongy with primary particles linked together in agglomerates of different sizes and shapes, which is in accordance with previous reports on combustion synthesis [31, 36].

The samples prepared with glycine had higher porosity than the PEG samples. Samples AP1 and AP2 (Figures5a and 5b) presented the highest degree of structural densification and particle size among all the prepared samples. Among the powders produced with glycine, the fuel-lean sample, AG3, presented the highest porosity with smaller particles compared to other concentrations (Figure6c).

The formation of the spongy features is attributed to the evolution of a large amount of gas during combus–tion [46]. The amount of oxygen involved in the reac–tion directly affects the speed and efficiency of the fuel reaction. For fuel-rich conditions, the fuel takes longer to react with oxygen from the atmosphere or does not react completely due to the limited infiltration. Longer exposure to elevated temperatures and slower gas release leads to larger mean size particle sizes and denser structures [40, 49]. For stoichiometric and lean conditions of glycine, the reactions were carried out under oxidizer conditions. Glycine has a small carbonic chain, and the presence of N and OH in the structure provides an intense and fast high-temperature combustion during ignition, which releases a high volume of gases [42]. Smaller crystallites and more porous structures were achieved for these compositions since the entry of oxygen is not a problem.

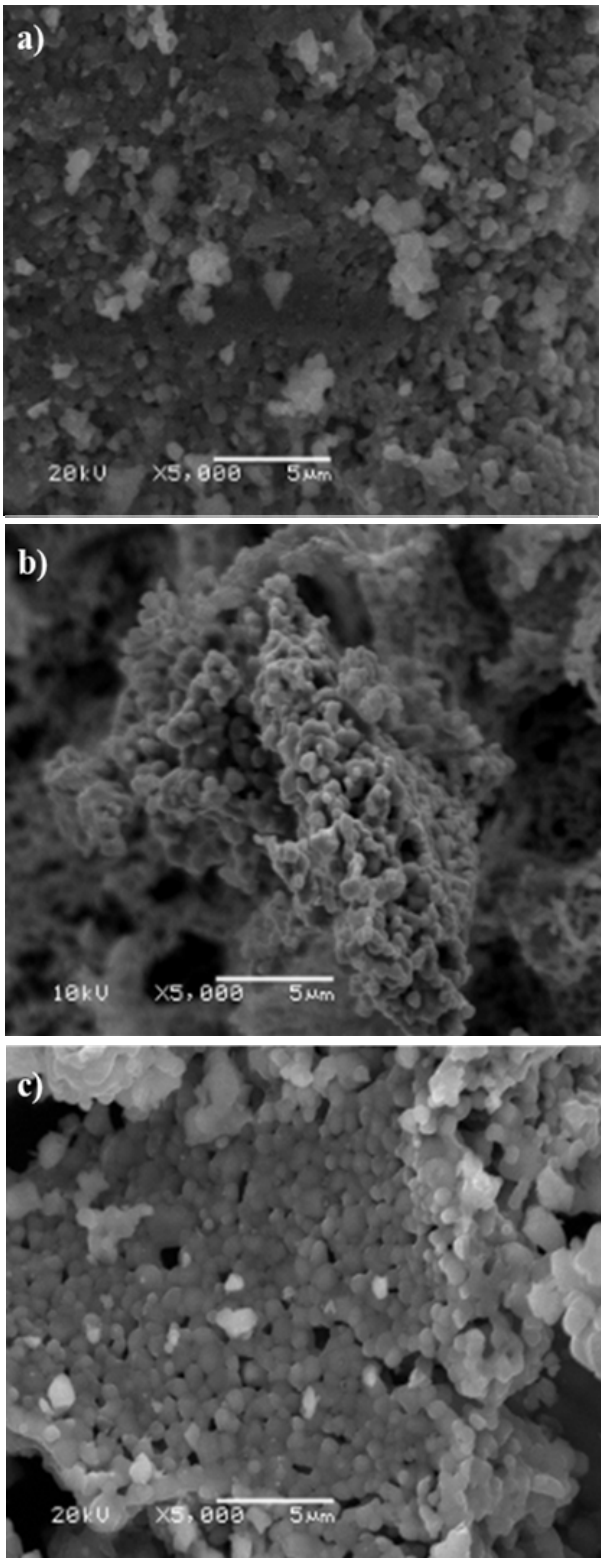

Figure5. SEM images of samples: a) AP1, b) AP2, c) AP3.

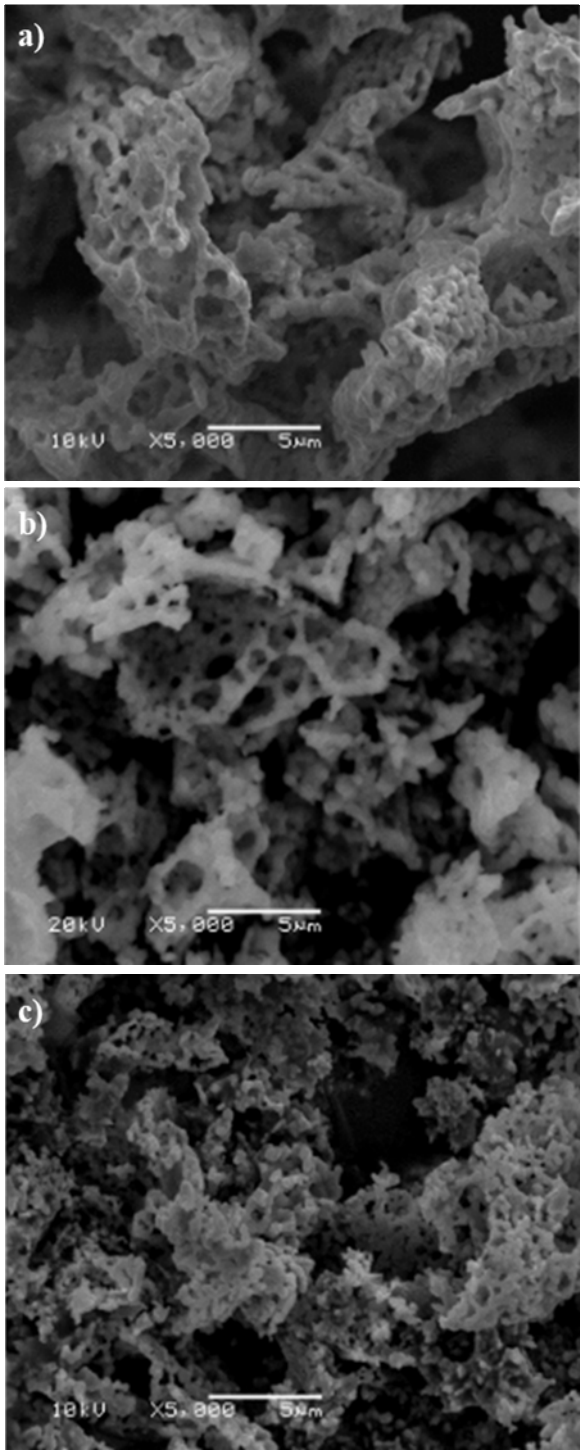

Figure6. SEM images of samples: a) AG1, b) AG2, and c) AG3.

The formation of the spongy features is attributed to the evolution of a large amount of gas during com–bustion [46]. The amount of oxygen involved in the reaction directly affects the speed and efficiency of the fuel reaction. For fuel-rich conditions, the fuel takes longer to react with oxygen from the atmosphere or does not react completely due to the limited infiltration. Longer exposure to elevated temperatures and slower gas release leads to larger mean size particle sizes and denser structures [40, 49]. For stoichiometric and lean conditions of glycine, the reactions were carried out under oxidizer conditions. Glycine has a small carbonic chain, and the presence of N and OH in the structure provides an intense and fast high-temperature combustion during ignition, which releases a high volume of gases [42]. Smaller crystallites and more porous structures were achieved for these compositions since the entry of oxygen is not a problem.

In the case of samples prepared with PEG, equation 2 shows that even for the stoichiometric composition, a high quantity of external oxygen is required for comp–lete fuel combustion. Also, the PEG has a long linear carbonic chain with the presence of OH at only the end of the chain. The combination of these factors causes the PEG ignition to take longer, and for the fuel-rich sample, the combustion may not even be completed. This explains the larger mean particles size and higher density of the foamy structures of these samples [50]

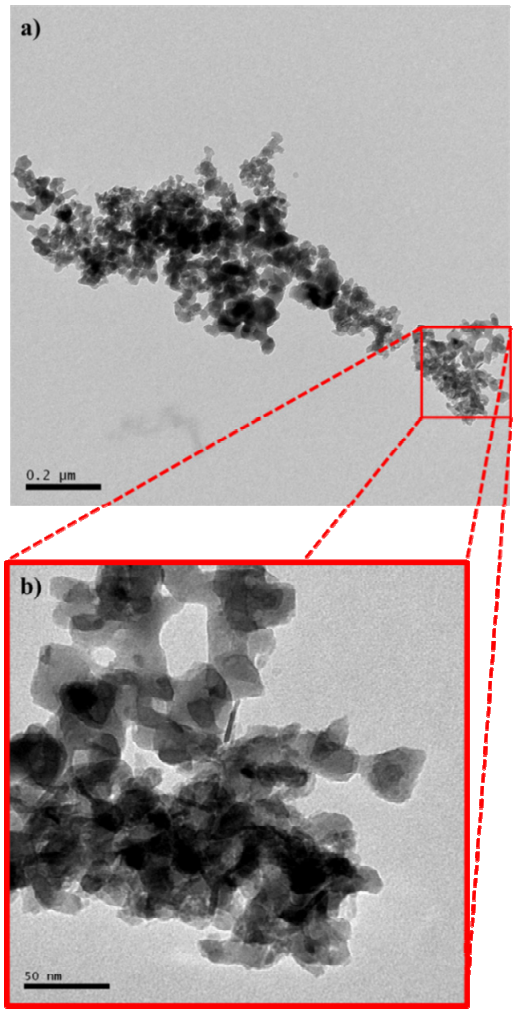

Figure 7. TEM images of the nanoparticles presentin sample AG3 a) 100kX and b) 500kX.

For iron-based catalysts, greater efficiency results from a higher surface area and degree of spinel inver–sion [11, 13]. Although the samples produced with PEG showed a high degree of spinel inversion due to the synthesis conditions, they presented large particles with low surface area, as well as the presence of a secondary periclase phase. The AG3 sample presented the smallest grain size with the highest surface area.

Despite not having the high inversion degree of the PEG samples, AG3 presented a higher degree of spinel inversion than the stoichiometric glycine sample, AG2. Due to the combination of these factors, AG3 is the

most appropriate sample for catalyst applications. Figure7 presents a TEM image of the AG3 particles. According to the TEM image, the particles have a size of approximately 50 nm with a high degree of agglo–meration. The observed particle size is in agreement with Scherrer's analysis (Figure4), which indicated crystals with an average size of 45 nm.

4. CONCLUSION

Nanostructured oxide catalysts were successfully obtained using different concentrations of glycine and PEG. The samples produced with PEG showed the highest degree of spinel inversion, but also the for–mation of a second phase, MgO. The use of glycine resulted in porous structures formed by high-purity nanoparticles. The fuel composition and concentration during the SCS proved to be crucial factors for obtai–ning high-quality iron-based powder catalysts. Glycine presented higher efficiency in the production of $MgFe_2O_4$ nanoparticles than PEG. The glycine-lean conditions provided the best results, which guaranteed fast and complete combustion during the SCS and resulting in structures with high surface area and redu–ced particle size.

ACKNOWLEDGEMENTS

The authors would like to thank the Coordination for the Improvement of Higher Education Personnel- CAPES for the financial support and the Microscopy and Microanalysis Center of Federal University of Rio Grande do Sul (CMM/UFRGS) for the technical support.

REFERENCES

[1] Lue, J. T.: Encyclopedia of Nanoscience and Nanotechnology, Physical Properties of Nanoma–terials, pp.1-47, 2007.

[2] Matija, L. R., Tsenkova, R. N., Miyazaki, M., Banba, K. andMucan, J. S.: Aquagrams: Water Spectral Pattern as Characterization of Hydro–genated Nanomaterial, FME Transactions, vol. 40, pp. 51-56, 2012.

[3] Debeljkovic, A., Veljic, V., Sijacki-Zeravcic, V., Matija, L. and Koruga, D.: Characterization of Materials for Commercial and New Nanophotonic Soft Contact Lenses by Optomagnetic Spectros–copy, FME Transactions, vol. 42, pp. 88-93, 2014.

[4] Fotouhi, M., Saghafi, H., Brugo, T., Minak, G., Fragassa, C., Zucchelli, A., Ahmadi, M.: Effect of PVDF nanofibers on the fracture behavior of com–posite laminates for high-speed woodworking mac–hines, Proceedings of the Institution of Mechani–cal Engineers, Part C: Journal of Mechanical Engi–neering Science, vol. 231, no. 1, pp. 31-43, 2017.

[5] Fragassa, C.: Effect of Natural Fibers and Bio-Resins on Mechanical Properties in Hybrid and Non-Hybrid Composites, Proceedings of the 8th Conference on Times of Polymers & Composites: From Aerospace to Nanotechnology. American Institute of Physics (AIP). 19-23th June, Ischia (Italy). AIP Conference Proceedings, Vol. 1736, No. 4949693; doi: 10.1063/1.4949693, 2016.

[6] Prieto, G., Tüysüz, H., Duyckaerts, N., Knossalla, J., Wang, G-H. Schüth, F.: Hollow Nano and Microstructures as Catalysts, Chem. Rev., Vol. 116, No. 22, pp. 14056-14119, 2016.

[7] Sharma, N., Ojha, H., Bharadwaj, A. Pathak, P.: RSC Advances Preparation and catalytic applications of nanomaterials: a review, RSC Adv., Vol. 5, pp. 53381-53403, 2015.

[8] Rao, C. N. R.,Müller, A. and Cheetham, A. K.: The Chemistry of Nanomaterials: Synthesis, Properties, and Applications, Wiley, Vol. 2,pp.1-764, 2004.

[9] Das, H.et al.: Impact of acidic catalyst to coat superparamagnetic magnesium ferrite nanoparticles with silica shell via sol–gel approach, Advanced Powder Technology, Vol. 27, pp. 541-549, 2016.

[10] Kobayashi, T.: Cancer hyperthermia using magne–tic nanoparticles, Biotechnol. J., Vol. 6, pp.1342-1347, 2011.

[11] Nonkumwong, J., Pakawanit, P., Wipatanawin, A., Jantaratana, P., Ananta, S., Srisombat, L.: Synthesis and cytotoxicity study of magnesium ferrite-gold core-shell nanoparticles,Materials Science and Engineering C, Vol. 61, pp.123-132, 2016.

[12] Fragassa, C., Berardi, L. and Balsamini, G.: Magnetorheological fluid devices: an advanced solution for an active control on the wood manu–facturing process. FME Transactions, Vol 44, No. 4, pp. 333-339, 2016.

[13] Reddy, D. H. K.,Yun, Y-S.: Spinel ferrite magnetic adsorbents: Alternative future materials for water purification?, Coordination Chemistry Reviews, Vol. 315, pp. 90-111, 2016.

[14] Gruneis, A.,Rummel, M.H., Kramberger, C., Barreiro, A., Pichler, T., Pfeiffer, R.,Kuzmany, H., Gemming, T. andBuchner, B.: High-quality double wall carbon nanotubes with a defined diameter distribution by chemical vapor deposition from alcohol, Carbon, Vol. 44, pp.3177-3182, 2006.

[15] Wang, Y., Wei, F., Luo, G., Yu, H. and Gu, G.: The large-scale production of carbon nanotubes in a nano-agglomerate fluidized-bed reactor, Chemical Physics Letters, Vol. 364, pp.568-572, 2002.

[16] Ning, G., Wei, F., Wen, Q.,Luo, G., Wang, Y., Jin, Y.:Improvement of Fe/MgO Catalysts by Calcination for the Growth of Single- and Double-Walled Carbon Nanotubes, J. Phys. Chem. B, Vol. 110, No. 3 pp.1201-1205, 2006.

[17] Li, Q. W.et al.: A scalable CVD synthesis of high-purity single-walled carbon nanotubes with porous MgO as support material, J. Mater. Chem., Vol.12, No. 4, pp.1179-1183, 2002.

[18] Zhang, Q., Zhao, M., Huang, J., Qian, W. Wei, F.: Selective Synthesis of SSingle/Double/Multi-walled Carbon Nanotubes on MgO-Supported Fe Catalyst, Chin J Catal., Vol .29, No. 11, pp. 1138-1144, 2008.

[19] Wang, Y., Wei, F., Luo, G., Yu, H. and Gu, G.: The large-scale production of carbon nanotubes in a

nano-agglomerate fluidized-bed reactor, Chemical Physics Letters, Vol. 364,pp. 568-572, 2002.

[20] Kaur, N. and M. Kaur, M.: Comparative studies on the impact of synthesis methods on structural and magnetic properties of magnesium ferrite nanoparticles, Process. Appl. Ceram., Vol. 8, No. 3, pp. 137-143, 2014.

[21] Wang, Z., Lazor, P., Saxena, S.K. O'Neill, H.S. C.: High-pressure Raman spectroscopy of ferrite MgFe2O4, Mater. Res. Bull., Vol. 37, No. 9, pp. 1589-1602, 2002.

[22] Zhang, Z.J., Wang, Z.L., Chakoumakos, B.C. and Yin, J.S.: Temperature Dependence of Cation Distribution and Oxidation State in MagneticMn - Fe Ferrite Nanocrystals, Vol. 7863, No. 15, pp. 1800-1804, 1998.

[23] Antao, S.M., Hassan, I.and Parise, J.B.: Cation ordering in magnesioferrite, $MgFe_2O_4$, to 982°C using in situ synchrotron X-ray powder diffraction, Am. Mineral., Vol. 90, No. 1, pp. 219-228, 2005.

[24] Xavier, C.S., Candeia, R.A., Bernardi, M.I.B., Lima, S.J.G., Longo, E., Paskocimas, C.A., Soledade, L. E. B.,Souza, A.G. and Santos, I.M.G.: Effect of the modifier ion on the properties of $MgFe_2O_4$ and $ZnFe_2O_4$ pigments, J. Therm. Anal. Calorim., Vol. 87, No. 3, pp. 709-713, 2007.

[25] Tilley, R. J. D.: Understanding Solids, John Wiley & Sons Ltd, England, 2004.

[26] Issa, B., Obaidat, I. M., Albiss, B. A. and Haik, Y.: Magnetic Nanoparticles: Surface Effects and Properties Related to Biomedicine Applications, Int. J. Mol. Sci., Vol.14, pp. 21266-21305, 2013.

[27] Huang, Y. et al.: Synthesis of $MgFe_2O_4$ nanocrystallites under mild conditions, Mater. Chem. Phys., Vol. 97, No. 2-3, pp. 394-397, 2006.

[28] Castro, S., Gayoso, M., Rodríguez, C.: A Study of the Combustion Method to Prepare Fine Ferrite Particles, J. Solid State Chem, Vol. 134, No. 2, pp. 227-231, 1997.

[29] Patil, K.C., Aruna, S.T. and Mimani, T.: Combustion synthesis: An update, Curr. Opin. Solid St Mat Sci Vol. 6, No. 6, pp. 507-512, 2002.

[30] Kikukawa, N. et al.: Synthesis and magnetic properties of nanostructured spinel ferrites using a glycine-nitrate process, J. Magn. Mater., Vol. 284, No. 1-3, pp. 206–214, 2004.

[31] Xue, H., Li, Z., Wang, X. and Fu, X.: Facile synthesis of nanocrystalline zinc ferrite via a self-propa–gating combustion method, Mater. Lett., Vol. 61, No. 2, pp. 347–350, 2007.

[32] Satyanarayana, L., Reddy, K. M. and Manorama, S. V.: Nanosized spinel NiFe2O4: A novel material for the detection of liquefied petroleum gas in air, Mat Chem Phys, Vol. 82, No. 1, pp. 21-26, 2003.

[33] Ilić, Z., Rašuo, B., Jovanović, M., Janković, D.: Impact of Changing Quality of Air/Fuel Mixture during Flight of a Piston Engine Aircraft with Respect to Vibration low Frequency Spectrum, FME Transactions, 41(1), pp. 25-32, 2013.

[34] Da Dalt, S., Takami, A.S., Volkmer, T.M., Sousa, V.C. Bergmann, C.P.: Magnetic and Mössbauer behavior of the nanostructured $MgFe_2O_4$ spinel obtained at low temperature, Powder Technol., Vol. 210, No. 2, pp. 103-108, 2011.

[35] Da Dalt, S., Takimi, A.S., Sousa, V.C. Bergmann, C.P.: Magnetic and Structural Characterization of Nanostructured $MgFe_2O_4$ Synthesized by Combu–stion Reaction, Part. Sci. Technol., Vol. 27, No. 6, pp. 519-527, 2009.

[36] Dinka P. and Mukasayan, A.:In situ preparation of Oxide-based Supported Catalysts by Solution Combustion Synthesis, J. Phys. Chem. B, Vol. 109, pp. 21627-21633, 2005.

[37] Sousa, V.C.et al.: Combustion synthesized ZnO powders for varistor ceramics, Int. J. Inorg. Mater., Vol. 1, pp. 235-241, 1999.

[38] Patil, K.C., Hegde, M.S., Rattan, T.and Aruna, S.T.:Chemistry of Nanocrystalline Oxide Mate–rials. World Scientific, 2008.

[39] Alves, A.K., Bergmann, C.P. and Berutti, F.A.: Combustion Synthesis, in: Alves, A.K., Bergmann, C.P. and Berutti (Eds.): Novel Synthesis and Cha–racterization of Nanostructured Materials, Sprin–ger, pp. 11–22, 2013

[40] González-Cortés, S.L. Imbert, F.E.: Fundamentals, properties and applications of solid catalysts prepared by solution combustion synthesis (SCS), App Cat A Gen, Vol.452, pp.117-131, 2013.

[41] Jain S.R., Adiga, K.C. and Pai Verneker, V.R.: A new approach to thermochemical calculations of condensed fuel-oxidizer mixtures, Combust. Flame, Vol. 40, pp. 71-79, 1981.

[42] Jovanović, R., Rašuo, B., Stefanović, P., Cvetinović, D., Swiatkowski, B.: Numerical investigation of pulverized coal jet flame characteristics under different oxy-fuel conditions, International Journal of Heat and Mass Transfer, Vol. 58, Issues 1–2, March 2013, pp. 654-662.

[43] Saito, G., Nakasugi, Y., Sakaguchi, N., Zhu, C. and Akiyama, T.: Glycine e nitrate-based solution-combustion synthesis of $SrTiO_3$, J Alloys and Compounds, Vol. 652, pp. 496–502, 2015.

[44] Lima, M.D., De Andrade, M.J., Locatelli, A., Balzaretti, N., Nobre, F., Bergmann, C.P. and Roth, S.: The effect of the combustible agents on the synthesis of Fe-Mo/MgO catalysts for the production of carbon nanotubes, Phys. Status Solidi Basic Res., Vol. 244, No. 11, pp. 3901-3906, 2007.

[45] Zampiva, R.Y.S., Kaufmann Junior, C.G., Pinto, J. S.,Panta, P.C.,Alves, A.K. and Bergmann, C.P.: 3D CNT macrostructure synthesis catalyzed by MgFe2O4 nanoparticles-A study of the surface area and spinel inversion influence, Appl. Surf. Sci., Vol. 422, pp. 321-330, 2017.

[46] Effenberg, G., Ilyenko, S.: Ternary Alloy Systems Phase Diagrams, Crystallographic and Thermo–dynamic Data, Springer Berlin Heidelberg, German, 2008.

[47] Ries, H. E.et al.: Surface Area of Catalysts, Ind. Eng. Chem., Vol. 37, No. 4, pp. 310-317, 1945.

[48] Rioux, R.M. et al.: High-Surface-Area Catalyst Design: Synthesis, Characterization, and Reaction Studies of Platinum Nanoparticles in Mesoporous SBA-15 Silica, J. Phys. Chem. B, Vol. 109, pp. 2192-2202, 2005.

[49] Toniolo, J.C., Bonadiman, R., Oliveira, L.L., Hohemberger, J.M.and Bergmann, C.P.: Synthesis of Nanocrystalline Nickel Oxide Powders via Glycine-Nitrate Combustion, No. 3, pp. 1–7, 2005.

[50] Gao, Y., Meng, F., Cheng, Y. and Li, Z.: Influence of fuel additives in the urea-nitrates solution combustion synthesis of Ni-Al2O3 catalyst for slurry phase CO methanation, Appl. Catal. A Gen., Vol. 534, pp. 12-21, 2017.

УТИЦАЈ САСТАВА ГОРИВА И ОДНОС ГОРИВА/ОКСИДАТОРА НА СИНТЕЗУ РАСТВОРА САГОРЕВАЊА НАНОДЕЛИЋА КАТАЛИЗАТОРА MgF_e2O_4

Р. Зампива, К. Кауфман, А. Алвес, К. Бергман

Синтеза сагоревања раствора (SCS) широко се примјењује на производњу оксидних катализатора захваљујући могућности производње високо чистих и хомогених наноструктурних праха по ниској цени. Што је мања честица и што је већа површина, ефи–касније је катализатор праха. За катализаторе на бази гвожђа као што су ферити, степен инверзије спинела је још један фактор који утиче на активност катализатора. У SCS-у, величина честица, површина и степен инверзије спинела су фундаментално пове–зани са промењљивим процесима као што су састав горива и однос горива/оксидатора.

Са тим у вези је проучена примена глицерина и полиетилен гликола - 200 молекулске масе (PEG 200) као горива и утицај односа горива/оксидатора у SCS-у $MgFe_2O_4$ каталитичких наночестица. Мор–фологија и састав производа су систематски карактерисани рентгенском дифракцијом, микро–скопском анализом и специфичном површином. Резултати указују на производњу наночестица високе чистоће са повишеном површинском повр–шином, која је добијена са ниским концентра–цијама глицина и широким распоном величине честица који зависе од састава горива и његове концентрације.